Thermostability of the Foot-and-Mouth Disease Virus Capsid Is Modulated by Lethal and Viability-Restoring Compensatory Amino Acid Substitutions

Silvia López-Argüello,[a] Verónica Rincón,[a] Alicia Rodríguez-Huete,[a] Encarnación Martínez-Salas,[a] Graham J. Belsham,[b] Alejandro Valbuena,[a] Mauricio G. Mateu[a]

[a]Centro de Biología Molecular Severo Ochoa (CSIC-UAM), Universidad Autónoma de Madrid, Madrid, Spain
[b]National Veterinary Institute, Technical University of Denmark, Kalvehave, Denmark

ABSTRACT Infection by viruses depends on a balance between capsid stability and dynamics. This study investigated biologically and biotechnologically relevant aspects of the relationship in foot-and-mouth disease virus (FMDV) between capsid structure and thermostability and between thermostability and infectivity. In the FMDV capsid, a substantial number of amino acid side chains at the interfaces between pentameric subunits are charged at neutral pH. Here a mutational analysis revealed that the essential role for virus infection of most of the 8 tested charged groups is not related to substantial changes in capsid protein expression or processing or in capsid assembly or stability against a thermally induced dissociation into pentamers. However, the positively charged side chains of R2018 and H3141, located at the interpentamer interfaces close to the capsid 2-fold symmetry axes, were found to be critical both for virus infectivity and for keeping the capsid in a state of weak thermostability. A charge-restoring substitution (N2019H) that was repeatedly fixed during amplification of viral genomes carrying deleterious mutations reverted both the lethal and capsid-stabilizing effects of the substitution H3141A, leading to a double mutant virus with close to normal infectivity and thermolability. H3141A and other thermostabilizing substitutions had no detectable effect on capsid resistance to acid-induced dissociation into pentamers. The results suggest that FMDV infectivity requires limited local stability around the 2-fold axes at the interpentamer interfaces of the capsid. The implications for the mechanism of genome uncoating in FMDV and the development of thermostabilized vaccines against foot-and-mouth disease are discussed.

IMPORTANCE This study provides novel insights into the little-known structural determinants of the balance between thermal stability and instability in the capsid of foot-and-mouth disease virus and into the relationship between capsid stability and virus infectivity. The results provide new guidelines for the development of thermostabilized empty capsid-based recombinant vaccines against foot-and-mouth disease, one of the economically most important animal diseases worldwide.

KEYWORDS capsid, foot-and-mouth disease virus, protein engineering, thermal stability, vaccine

Successful infection of cells by any virus depends on an appropriate balance between capsid conformational stability and dynamics (1–4). A viral capsid protects the genome by maintaining extracellular integrity, but at the same time it may be prone to change its conformation or disassemble during certain steps of the infection process, including entry into a host cell and uncoating of the viral nucleic acid. In response to such conflicting selective constraints, many viruses have evolved a meta-

stable capsid whose conformation and/or integrity is modulated by specific factors during the infectious cycle (3).

Interestingly, the capsids of some viruses (e.g., certain picornaviruses) are particularly prone to conformational rearrangements or dissociation when subjected to physical or chemical stress (4–6). This lability may be disadvantageous for survival in the extracellular environment, but it may be required for infection of susceptible cells. A low enough thermodynamic stability may avoid kinetic trapping during capsid assembly (7). Also, a higher activation free energy barrier between the capsid native state and a conformationally altered or disassembled state could be difficult to overcome by the specific factors that trigger such a reaction during infection (8).

Identification of the structural determinants of the delicate balance between capsid stability and instability may provide a deeper understanding of virus morphogenesis and genome uncoating, two relatively poorly understood steps of the virus infection cycle (4, 7, 9, 10). This knowledge could be applied to the development of new antiviral drugs and for improvement of the stability of virus particles for nanobiotechnological or biomedical purposes (11–14), including the production of thermostable vaccines (5).

An important viral pathogen that is remarkably prone to disruption by physical or chemical treatments is foot-and-mouth disease virus (FMDV), a member of the picornavirus family (15, 16). The virion contains a single-stranded RNA genome enclosed in a P=3 (T=1) icosahedral capsid (17, 18) (Fig. 1A and B). The capsid is formed from 60 copies of each of three virus proteins (VP1, VP2, VP3) and a small, internal polypeptide (VP4) that are produced by proteolytic processing of the P1-2A capsid precursor. One copy of each VP makes a protomer, five protomers make a pentamer, and 12 pentamers associate to form the capsid (Fig. 1A to C). Mild acidification of the FMDV virion (both *in vitro* and within endosomes *in vivo*) results in uncoating of the genome and dissociation of the capsid into pentamers (6, 19–21). FMDV virions and capsids are also quite labile and prone to dissociation into pentamers even at neutral pH and low temperatures (5).

Paradoxically, FMDV thermolability is a serious problem for the control of foot-and-mouth disease (FMD) (22). FMD is one of the economically most important animal diseases worldwide (23, 24). Vaccination is an essential strategy to combat FMD in countries where this disease is enzootic. Current FMD vaccines are based on chemically inactivated but structurally intact virions (25). Maintaining viral particle integrity is essential for maintaining vaccine potency (26, 27). Thus, one important shortcoming of these vaccines comes from the weak stability of FMDV virions against heat-induced dissociation into the poorly immunogenic pentamers. This feature imposes the necessity of keeping a strict cold chain from manufacturing to vaccination. Unfortunately, the infrastructure and climate of many developing countries where FMD is enzootic make it difficult to maintain a fail-safe cold chain (22). The weak thermostability of the FMDV capsid is also a problem for the ongoing development of novel FMD vaccines based on recombinant empty capsids (28–30; recently reviewed in references 5 and 31). FMDV empty capsids used as vaccines would avoid the risks associated with the production of infectious virus and could facilitate differentiation between infected and vaccinated animals, but they are even less thermostable than virions (26).

The demand to improve FMDV thermostability for production of current, virion-based and (eventually) empty capsid-based vaccines that are less dependent on a strict cold chain led our group to undertake the engineering of FMDV virions with increased thermal stability. As a result, Mateo et al. (32) first provided a proof of concept that FMDVs could be genetically modified to drastically increase their stability against heat-induced dissociation into pentamers while still preserving (i) antigenic specificity, (ii) full virus infectivity and enough genetic stability (needed for vaccine production), and (iii) normal sensitivity to chemical inactivation (to avoid an increased risk of deficient inactivation). Since then, we and other researchers, working with different FMDV serotypes and using diverse approaches to design stabilizing mutations, have engineered several thermostabilized virions (32–34) or empty capsids (35, 36). Unfortunately, some mutant viruses were not viable, and only some of the viable, thermo-
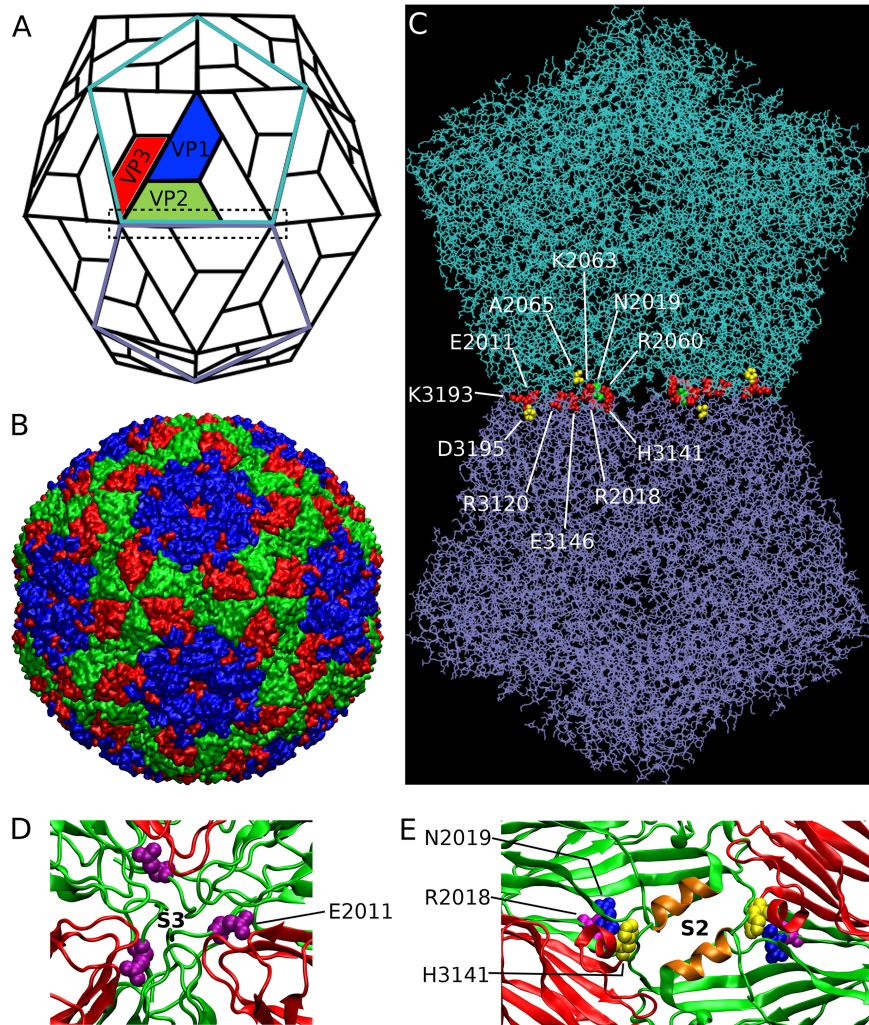
FIG 1 Structure of FMDV indicating residues at the interpentamer interfaces selected for analysis of capsid thermostability. (A) Scheme of the icosahedral FMDV capsid. A biological protomer consisting of VP1 (blue), VP2 (green), VP3 (red), and the internal polypeptide VP4 (not visible) is shown in color. Two neighboring pentamers are delineated in cyan or violet. The interface between these two pentamers is enclosed within a dashed rectangle. (B) Atomic structure of FMDV (C-S8c1) (37) in the same orientation shown in panel A. VP1, VP2, and VP3 are colored blue, green and red, respectively. (C). Wire frame atomic model of two neighboring pentamers corresponding to the color-contoured pentamers in panel A. The amino acid residues at the interpentamer interface whose role in capsid thermostability was analyzed here are represented using space-filling models and color coded as follows: yellow, D3195 and A2065; green, N2019; and red, other tested, charged residues. One of each pair of equivalent residues belonging to either pentamer has been labeled. (D, E) Close-up ribbon models of two regions around interpentamer interfaces. VP2 and VP3 are colored green and red, respectively. (D) The β-annulus at each capsid 3-fold axis (S3) joining 3 pentamers together. Residue E2011 is represented using a magenta space-filling model. (E) A region around the capsid 2-fold axis (S2) at the center of each interpentamer interface. At the right and left, two equivalent β-sheets (each formed by two β-strands from VP2 from one pentamer [green] and five β-strands from VP3 from the neighboring pentamer [red]) contribute to join the two pentamers together. At the center there are two equivalent α-helices (orange) from symmetry-related VP2 subunits across a capsid 2-fold axis (S2). Residues R2018, H3141, and N2019 are represented using magenta, yellow, and blue space-filling models, respectively.

stabilized mutant viruses showed normal infectivity and adequate genetic stability, required for vaccine production (32–34).

The present study was undertaken to understand better the relationships between virus capsid structure and thermostability and between capsid thermostability and viral infectivity, with a view to further contribute to the rational design of improved FMD vaccines. We analyzed the effects on the thermostability of the FMDV capsid of substitutions of charged amino acid residues relevant for virus infectivity and located

TABLE 1 Tested FMDV capsid mutations that remove charged groups at interpentamer interfaces

| Mutation[a] | Interpentamer interaction(s) removed[b] | | van der Waals contacts[c] | Virus infectivity titer relative to wt control[d] |
	Ionic	H bond		
E2011A	K3118 (3.8)		7 (2)	$<3 \times 10^{-5}$
R2018A		N1017, Y1018	4 (2)	$<3 \times 10^{-5}$
R2060A	E2213	E2213, H3141, C3142	3 (0)	$<3 \times 10^{-5}$
K2063A	E3146	H3144, E3146	12 (3)	0.15 (forw. mut.)
R3120A	E2108 (4.8)	S2024, T2025, T2026, T2110	3 (1)	2×10^{-3}
H3141A	Helix dipole		6 (3)	$<3 \times 10^{-5}$
E3146A	K2063	K2063	4 (1)	0.22 (revertant)
K3193A		A2192	8 (3)	2×10^{-4}

[a]For each substituted amino acid residue, the first digit indicates the protein (either VP2 or VP3) and the last three digits indicate the amino acid position according to the normalized FMDV capsid numbering used in the file for FMDV C-S8c1 (PDB accession number 1FMD) (37).

[b]The cutoff distances considered were 3.5 Å for hydrogen bonds and for ionic bonds participating in salt bridges; 5 Å for medium-range ionic interactions (the distance between interacting groups is indicated); and 0.5 Å longer than the sum of the van der Waals (vdW) radii of the two interacting atoms for van der Waals interactions.

[c]For ionic or hydrogen bonds, the interacting residue is indicated. For van der Waals interactions, the total number of contacts and (in parentheses) the number of carbon-carbon contacts removed are indicated.

[d]Viral titers were taken from reference 38. The average absolute titer obtained for the wt virus was 1.6×10^6 PFU/ml (at 45 h postransfection). Viral progeny populations were sequenced; the site-directed mutation was preserved, and no other mutations were found, except for K2063A and E3146A, for which a different forward mutation (forw. mut.) or a reversion (revertant), respectively, had been fixed, indicating the lethality of the original mutations (see the text).

at or close to the interpentamer interfaces (Fig. 1C). In addition, we studied whether capsid thermostability may be modulated by charge-compensating mutations that restored the FMDV viability lost upon removal of certain charged groups at the interpentamer interfaces.

RESULTS

Selection of charged residues at interpentamer interfaces in the FMDV capsid for assessing their role in capsid assembly or thermostability. Analysis of the crystal structure of the FMDV C-S8c1 virion (37) revealed that 42 side chains per protomeric subunit are involved in interpentamer noncovalent interactions (38) (this number takes into account only those side chains in which the interpentamer interactions involve atoms beyond the β-carbon). Of these 42 side chains, as many as 18 (43%) contain chemical groups that are charged at close to neutral pH. Three of these 18 groups are imidazoles (H2021, H3141, H3144). These groups are assumed to be positively charged most of the time even at neutral pH, because the pK_a in free histidine (pK_a, ~6.8) is frequently raised in folded proteins due to the proximity of negatively charged carboxylates (39, 40); the same is also observed in the FMDV capsid.

Individual removal by substitution to alanine of 15 out of these 18 charged groups (83% of cases) was lethal for the virus (no detectable progeny virus; 10 cases) or drastically reduced its infectivity (by 3 to 4 orders of magnitude; 5 cases) (38). It seemed possible that some of these charged side chains at the interpentamer interfaces in the FMDV capsid which are required for virus infectivity could modulate its assembly and/or thermal stability against dissociation into pentameric subunits. We chose 8 of these 18 charged side chains (44%) for analysis as a representative sample that considered (i) differently charged residues (either positively [Lys, Arg, His] or negatively [Glu] charged), (ii) residues located in different structural elements along the interpentamer interface, and (iii) residues that were involved in different types of noncovalent interactions (Table 1 and Fig. 1C).

Deleterious amino acid substitutions at interpentamer interfaces involving charge removal have no substantial effect on expression and proteolytic processing of the capsid polyprotein. The 8 mutations chosen (and additional mutations, specified below) (Table 1) were individually introduced into the P1-2A-coding region of FMDV C-S8c1 contained within recombinant plasmid pL1-1 (see Materials and Methods). For expression of capsid proteins and assembly of capsids (wild type [wt] and mutants), a dedicated vaccinia virus (VV)-based protein expression system was used as described in Materials and Methods. Cells from the same batch were transfected with
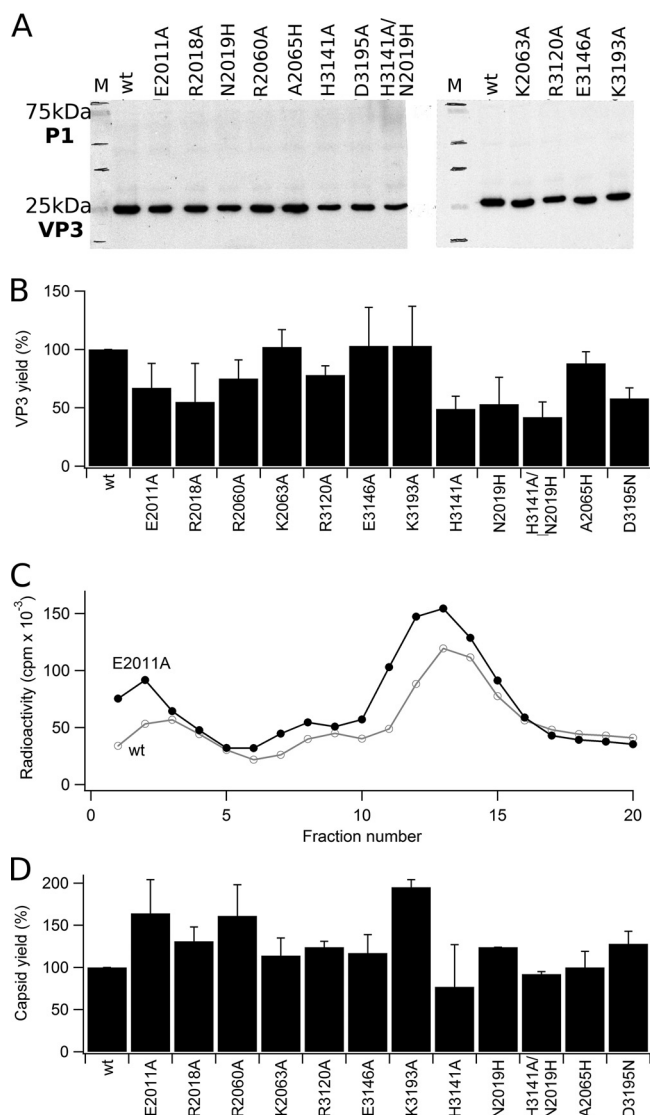
FIG 2 Capsid protein expression and processing and capsid assembly. (A) Representative results of Western blot assays to compare the expression and processing of wt and mutant capsid protein VP3 (indicated by the corresponding labels). Lanes labeled M correspond to molecular weight markers. The positions of unprocessed polyprotein P1-2A and the processed product VP3 are indicated. (B) Percent yields of the mutant mature capsid protein VP3s relative to the yield of the wt control. For each mutant, the averaged value obtained from 2 independent experiments and the corresponding error bar (standard deviation) are indicated. (C) A representative example of the centrifugation analysis carried out to estimate relative capsid yields (in this case, the yield of mutant capsid E2011A is compared to that of the wt capsid, used as the internal control in the same experiment). The larger peaks correspond to assembled capsids; the minor peaks on the left correspond to free pentameric subunits. (D) Percent yields of different mutant assembled capsids relative to the yield of the wt control. For each mutant for which results are presented in panels B and D, the averaged value obtained from 2 independent experiments and the corresponding error bar (standard deviation) are indicated.

equal amounts of wt or mutant pL1-1 plasmids and an appropriate amount of the pSKRH-3C plasmid containing the coding region for the FMDV (serotype A10) 3C protease, which is able to process the capsid precursor of C-S8c1. The yield of expressed and processed capsid proteins obtained with each mutant and the wt control was compared in quantitative immunoassays using a capsid protein (VP3)-specific monoclonal antibody (Fig. 2A). Average relative values obtained from two independent experiments (Fig. 2B) revealed that the tested amino acid substitutions had no major effects on the yield of processed capsid protein (average values were from ~50% lower to ~10% higher than those for the wt control).

Deleterious amino acid substitutions at interpentamer interfaces involving charge removal have no substantial effect on capsid assembly. Cells transfected with equal amounts of wt and mutant pL1-1 plasmids and with an appropriate amount of pSKRH-3C were then used to produce metabolically radiolabeled, assembled capsids as described in Materials and Methods. The ratio between the yield of each mutant capsid and that of the control wt capsid was estimated by measuring the radioactivity in the peak corresponding to assembled empty capsids (sedimentation coefficient, 75S) after centrifugation in analytical sucrose density gradients, as described in Materials and Methods (see one example in Fig. 2C). Average relative values obtained from two independent experiments (Fig. 2D) revealed that none of the substitutions led to any substantial reduction in capsid yield. In fact, clearly higher average yields were obtained for the E2011A, R2060A, and K3193A mutant capsids than for the control wt capsid. In the absence of further experiments, we are uncertain about why those mutants were obtained at higher yields. Differences in reactivity with the antibody used to detect denatured capsid protein VP3 in Western blot assays are unlikely, as in two of these three mutants the amino acid substitution was introduced in a different capsid protein (VP2). A higher capsid thermostability cannot explain these results either (see below). The differences could be related instead to a lower tendency of these mutant capsids to aggregate or suffer mechanical disruption during the analysis. Whatever the case, comparison of the results on protein expression and capsid yield showed that no tested amino acid substitution exerted a substantial negative effect on capsid assembly.

Some deleterious amino acid substitutions at interpentamer interfaces involving charge removal lead to a large increase in capsid thermostability. To determine, in a quantitative fashion, the role of specific charged groups at the interpentamer interfaces on the stability of the FMDV capsid against thermally induced dissociation, we concentrated especially on three particular residues because of their strategic locations (Fig. 1C to E). These were (i) residue E2011, which is located at a β-annulus formed by the N termini (Nt) of three VP2 subunits, which knits three pentamers together around each 3-fold symmetry (S3) axis in the capsid (37) (Fig. 1D); (ii) residue R2018, which is located at a β-hairpin in the VP2 Nt that, together with 4 β-strands of VP3 from a neighboring pentamer, participates in a β-sheet that crosses the interfaces between pentamers, holding them together (17, 37) (Fig. 1E); and (iii) residue H3141, which is located close to residue R2018; these two residues may establish, even at neutral pH, repulsive electrostatic interactions with the dipole of a neighboring α-helix (VP2 residues 2089 to 2098) located near each 2-fold symmetry (S2) axis in the capsid (Fig. 1E). It has been shown previously that H3141 contributes through repulsive electrostatic effects to the acid lability of FMDV and uncoating of its genome (17, 41–45).

Cells transfected with the mutant and control wt pL1-1 plasmids and the pSKRH-3C plasmid were used to produce metabolically radiolabeled, assembled capsids as described above. Protocols tested to obtain capsids with an adequate level of purity for quantitative analysis of thermostability involved a combination of steps. Trials included centrifugation through sucrose cushions, sucrose gradients, and/or CsCl density gradients; size exclusion chromatography in Sephacryl S-500HR or S-1000HR; and/or affinity chromatography. Two tested procedures worked the best. Method I involved centrifugation through a 20% sucrose cushion, followed by centrifugation through a 7.5% to 30% sucrose gradient and then through a CsCl density gradient and a final affinity chromatography step to remove nonassembled pentamers. This extensive procedure yielded fairly pure capsids, but the final yields were generally too low for analysis. Method II involved centrifugation through a 20% sucrose cushion, followed by centrifugation on a 7.5% to 30% sucrose gradient. This simplified procedure was adopted for obtaining reasonably pure capsids in sufficient yields for stability analysis. Figure 3 shows the presence of assembled capsids with the correct size and shape both in fairly pure preparations in which no pentameric subunits or conspicuous contaminants were detected (Fig. 3A) and also in the partially purified preparations (Fig. 3B) (see the enlarged images of single capsids in the corresponding insets).
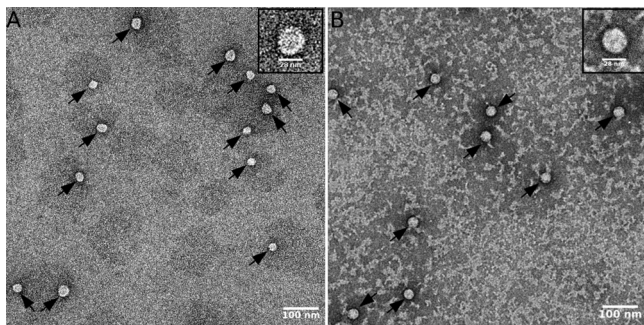
FIG 3 Electron micrographs of capsid preparations. (A) Capsids that had been extensively purified through method I. (B) Capsids that had been only partially purified. Arrows point to individual assembled capsids. (Insets) Enlarged images of single capsids to better assess size and shape. Scale bars are included.

Radiolabeled, purified E2011A, R2018A, or H3141A mutant and control wt capsids were tested for thermostability in parallel under the same conditions, as described in Materials and Methods. Capsids were incubated at 42°C and pH 7.5, and the percentage of intact capsids remaining after different incubation times was estimated by determining the radioactivity corresponding to the 75S peak after centrifugation in analytical sucrose density gradients. Two to four independent experiments were carried out for each mutant and the corresponding control wt, and the values obtained were averaged. The results (Fig. 4) revealed that substitution E2011A had no significant effect on capsid thermostability (Fig. 4A). In contrast, substitutions R2018A (Fig. 4B) and H3141A (Fig. 4C) had quite substantial thermostabilizing effects, as shown by their much lower dissociation rates at 42°C relative to the rate for the control wt capsid analyzed in parallel under the same conditions (Fig. 4), increasing the half-life by as much as ~5-fold for the H3141A mutant and even more for the R2018A mutant.

The role in capsid thermostability of 5 other interfacial charged groups also selected for analysis was not quantitatively determined due to the difficulty in obtaining sufficient amounts of adequately pure empty capsids. However, it was qualitatively assessed by using radiolabeled capsids that had been partially purified by centrifugation through sucrose cushions. Two independent experiments were carried out for each mutant and the wt control, and the values obtained were averaged. The results (Fig. 5) did not reveal any major stabilizing or destabilizing effect produced by any of the 5 mutations.

To sum up, the drastic deleterious effects on virus infectivity caused by individually removing different charged groups at the interpentamer interfaces in the FMDV capsid are not generally related to equally drastic changes in capsid protein expression or processing, capsid assembly, or (in most cases) capsid stability against thermal dissociation. In contrast, the charged side chains of R2018 and H3141, located close to the capsid 2-fold axes, are critical both for virus infectivity and for keeping the FMDV capsid in a state of weak thermal stability (even) at neutral pH.

Capsid thermostabilization by removing the imidazole group of H3141 can be reverted by introducing another imidazole nearby. We observed previously that when the amino acid substitution H3141A or R2018A was individually introduced into the virion, then infectivity was nearly abolished (38, 46). However, replication in transfected cells of viral RNA carrying either of those two substitutions repeatedly led to fixation in the genome of another mutation, resulting in a second-site substitution, N2019H. This mutation became dominant in the viral population and compensated for the lethal effect of the primary H3141A and R2018A substitutions, restoring virus viability (46). Remarkably, the N2019H compensatory substitution involved the introduction into the capsid of a positively charged group in a position that was spatially close to the positively charged side chains of H3141 and R2018 (Fig. 1E) that had been removed by the primary substitutions (46).
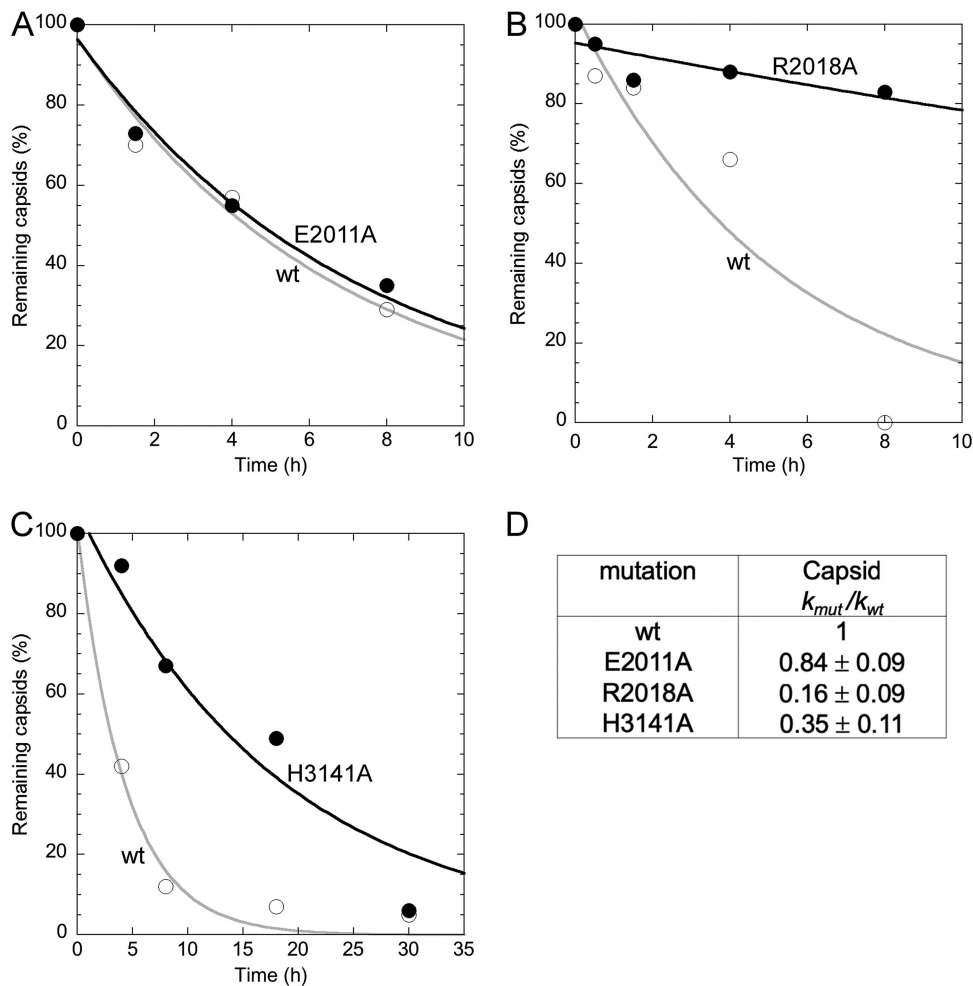
FIG 4 Thermal stability of purified E2011A (A), R2018A (B), and H3141A (C) mutant empty capsids containing charged-to-neutral (Ala) substitutions at the interpentamer interfaces (filled circles) relative to that of the wt empty capsid control (open circles). The percentages of intact capsids remaining after different incubation times in a representative experiment at 42°C are indicated in each case. Data were fitted to exponential decay processes, and the dissociation rate constants were obtained. The gray curve was obtained using the control wt capsid. (D) Ratios between the rate constant obtained for each mutant (k_{mut}) and the rate constant obtained for the wt control (k_{wt}). Values are averages and standard deviations obtained from 2 (E2011A and R2018A) or 4 (H3141A) independent experiments.

We reasoned that, if the lethal effect of the H3141A substitution was related to its capsid-thermostabilizing effect, restoration of virus viability by introducing the compensatory N2019H substitution may also reverse the thermostabilizing effect of the lethal substitution H3141A. We introduced the mutation encoding the N2019H substitution, alone or together with the H3141A change, into the pL1-1 plasmid and compared the effects of these mutations on capsid protein expression, capsid assembly, and capsid stability. Each mutant capsid and the control wt capsid were obtained, purified, and analyzed in parallel. These substitutions (H3141A, N2019H, and the double substitution H31341A/N2019H) had no major effect (average reduction, ~50%) on the yield of processed capsid protein (Fig. 2B) and no significant effect on the yield of assembled capsids (Fig. 2D).

The quantitative effects of those substitutions on the stability of the FMDV capsid against thermally induced dissociation (at pH 7.5) were then compared using purified radiolabeled capsids as described above. Four independent experiments testing the mutant capsids in parallel with the control wt capsid were performed, and the values obtained were averaged. The results (Fig. 6) revealed that (i) the H3141A capsid is much
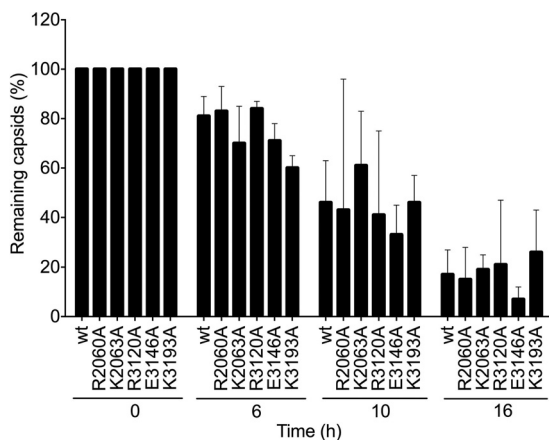
FIG 5 Thermal stability of 5 additional partially purified mutant empty capsids containing charged-to-neutral (Ala) substitutions at the interpentamer interfaces relative to that of the wt empty capsid control. The percentages of intact capsids remaining after different incubation times in a representative experiment at 42°C are indicated in each case. For each mutant, the average value obtained from 2 independent experiments and the corresponding error bar (standard deviation) are indicated.

more stable than the wt (the half-life increased by ~5-fold under the experimental conditions used), and the N2019H capsid was also substantially more stable than the wt (the half-life increased by ~2.5-fold); (ii) in contrast, the H3141A/N2019H capsid was only marginally more stable than the wt (the half-life increased by ~1.3-fold only).

To sum up, the results just described show that (i) the lethal H3141A primary substitution substantially stabilizes the FMDV capsid against heat-induced dissociation and (ii) the compensatory N2019H substitution that, in the context of H3141A, restores
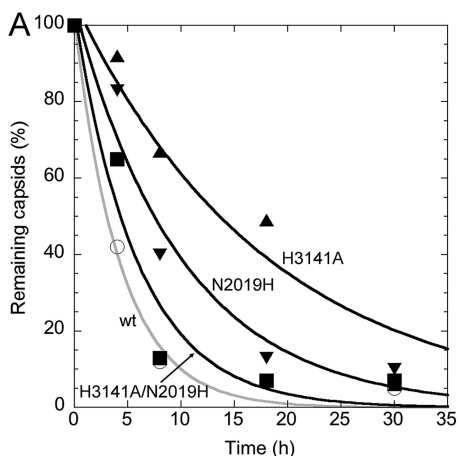
mutation	Capsid k_{mut}/k_{wt}
wt	1
H3141A	0.35 ± 0.11
N2019H	0.41 ± 0.17
H3141A/N2019H	0.63 ± 0.16

FIG 6 Thermal stability of purified mutant empty capsids containing the lethal charged-to-neutral substitution H3141A and/or the viability-restoring, charge-compensating substitution N2019H relative to that of the wt empty capsid control. (A) Percentage of intact capsids remaining after different incubation times at 42°C in a representative experiment. Open circles, wt capsids; filled triangles, mutant H3141A; filled inverted triangles, mutant N2019H; filled squares, mutant H3141A/N2019H. Data were fitted to exponential decay processes, and dissociation rate constants were obtained. The gray curve was obtained using the control wt capsids. (B) Ratios between the rate constant obtained for each mutant and the rate constant obtained for the wt control. Values are averages and standard deviations obtained from 3 (N2019H) or 4 (all other variants) independent experiments.

virus viability also reverses the capsid-stabilizing effect of H3141A leading to double-substituted H3141A/N2019H capsids with close to normal (wt) stability.

Amino acid substitutions involving charge variation thermostabilize virions and empty capsids to different degrees. In this study, we identified several single amino acid substitutions involving charge removal or introduction (H3141A, R2018A, and N2019H) that thermostabilize the FMDV empty capsid. In previous studies (32, 33), we identified other single substitutions that also involved charge variation and that thermostabilized the infectious FMDV virion, but they were located in a different region of each interpentamer interface (D2068N, E2086Q, D3134N, D3195N, and A2065H). We wondered whether the effects of these mutations on thermostability, so far analyzed on either the empty capsid or the virion, but not both, can occur irrespective of the absence or the presence of the negatively charged viral nucleic acid.

We asked, first, whether empty capsid-thermostabilizing substitutions involving charge variation may also stabilize the infectious RNA-filled virion. Unfortunately, the lethal nature of the capsid-thermostabilizing H3141A substitution made it impossible to test its effect on virion thermostability. However, the subsequent introduction of the secondary N2019H substitution led to a viable H3141A/N2019H double mutant virion. This fact provided the opportunity to analyze the effect on virion thermostability of the N2019H substitution both in the absence and in the presence of H3141A.

Mutations encoding the substitutions H3141A and N2019H, alone or combined, were introduced into a recombinant plasmid, pO1K/C-S8c1, that contains the full-length FMDV cDNA (47). Susceptible cells were transfected in the same experiment under the same conditions with equal quantities of wt or mutant RNA transcripts prepared from these plasmids, and FMDV virions with a C-S8c1 capsid (wt or mutant) were obtained (38, 48). As expected, the H3141A mutant virion was essentially not viable (infectious titer, <0.00007 that of the wt). In contrast, the H3141A/N2019H double mutant virion was infectious, as was the N2019H single mutant, albeit infectious virus progeny titers were reduced compared to those for the wt (the relative infectious titers were 0.016 ± 0.006 and 0.038 ± 0.004 that of the wt, respectively).

Sequencing of the entire capsid-coding region of the rescued progeny virus genomes revealed that the introduced mutations were still present and that no additional mutations had been fixed in the initial progeny virus populations. However, after further viral replication cycles (required to obtain sufficient amounts of purified virions for stability assays), additional mutations were detected in a large fraction of individual viral genomes in the populations (Q1195H was present in two independent amplifications of the H3141A/N2019H mutant, and V1015A was present in one amplification of the N2019H mutant).

The stability of the N2019H, N2019H (+V1015A), and H3141A/N2019H (+Q1195H) mutant virions against thermal dissociation (at pH 7.5) was then compared with that of the wt virion. Thermal dissociation assays were conducted as described above for empty capsids but using purified, radiolabeled virions. Two independent experiments were carried out for each mutant virus in parallel with the control wt virus, and the results were averaged (Fig. 7). The virions carrying the N2019H substitution (+V1015A) but not the H3141A change showed a stability similar to that of the wt. The virion carrying the H3141A/N2019H double substitution (+Q1195H) was even less stable than the wt. Thus, none of the viable combinations of substitutions led to virion thermostabilization. The presence of the accompanying mutations fixed during amplification of the viral populations did not allow us to establish whether the thermostability difference between empty capsids and virions carrying the N2019H substitution (either alone or together with H3141A) were related to the RNA contained in the virions.

Thus, we resorted to analyzing whether virion-thermostabilizing substitutions involving charge variations may also stabilize the empty capsid. We chose the A2065H and D3195N mutants as representative examples. The corresponding mutations were introduced into the pL1-1 plasmid, and the mutant and control wt capsids were obtained, purified, and analyzed in parallel. Neither of these substitutions had a
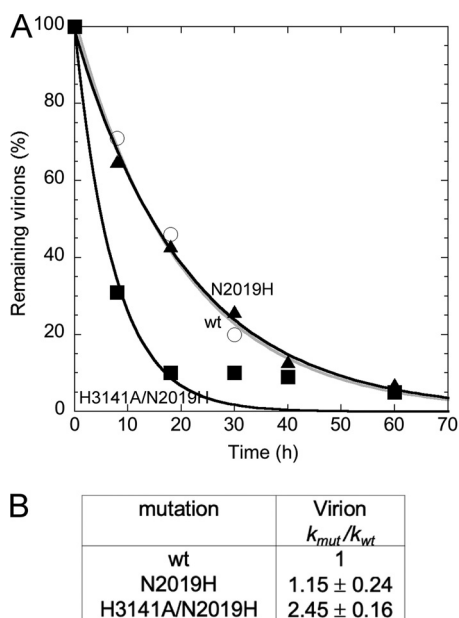
FIG 7 Thermal stability of purified mutant virions containing substitution N2019H alone (filled triangles) or together with the H3141A change (filled squares) relative to that of the wt virion control (open circles). The percentages of intact virions remaining after different incubation times at 42°C in a representative experiment are indicated. Data were fitted to exponential decay processes, and dissociation rate constants were obtained. The gray curve was obtained using the control wt capsids. The table indicates the ratios between the rate constant obtained for each mutant and the rate constant obtained for the wt control. Values are averages and standard deviations obtained from 2 or 3 independent experiments.

substantial effect on capsid protein expression and processing (Fig. 2B) or capsid assembly (Fig. 2C).

The stability of the A2065H and D3195N mutant empty capsids against thermally induced dissociation (at pH 7.5) was then determined using purified radiolabeled capsids as described above. Experiments were carried out for each mutant capsid in parallel with the control wt capsid. The results (Fig. 8) revealed that both A2065H and D3195N mutant empty capsids are more stable than the wt empty capsid. Thus, both substitutions stabilize FMDV particles irrespective of the presence or absence of the viral RNA. However, quantitative data for mutant A2065H (compare the results shown in Fig. 8 with those shown in reference 32) indicated that the thermostabilizing effect of this substitution may be rather less pronounced on the empty capsid than on the virion under similar conditions. To sum up, the presence of the viral RNA inside the FMDV capsid may modulate (i.e., increase, in the cases tested) the thermostabilizing effect of an amino acid substitution that involves charge variation close to the inter-pentamer interfaces.

No effect on capsid resistance against acid-induced dissociation of capsid-thermostabilizing substitutions. Finally, we compared, as described in Materials and Methods, the effects of mild acidification on the stability against dissociation of partially purified wt and mutant empty capsids carrying the capsid- and virion-thermostabilizing substitutions A2065H, D3195N, and H3141A. The results (Fig. 9) did not reveal a significant effect of any of these three mutations on capsid sensitivity to acid-induced dissociation.

DISCUSSION

Charged residues at different locations along the interpentamer interfaces preserve the high thermolability of the FMDV capsid even at neutral pH. In a previous study (33), we identified a cluster of solvent-exposed, negatively charged residues (D2068, E2086, D3134, D3195) that contribute to limit the thermostability of the FMDV virion (even at neutral pH) by establishing electrostatic repulsions between
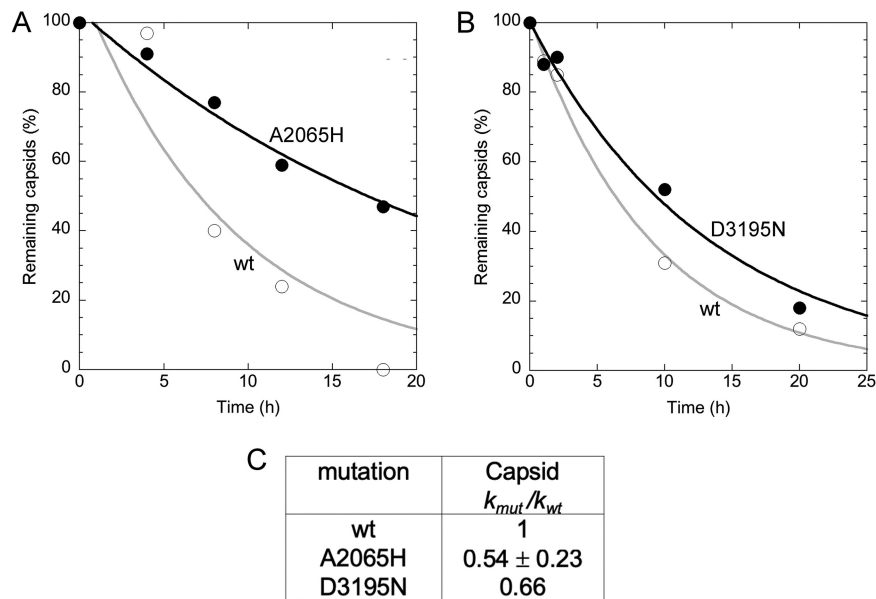
FIG 8 Thermal stability of purified mutant empty capsids containing virion-stabilizing, neutral-to-charged A2065H or charged-to-neutral D3195N substitutions relative to that of the wt empty capsid control. (A, B) The percentages of intact capsids remaining after different incubation times at 42°C in a representative experiment are indicated. Open circles, wt capsid; filled circles, A2065H mutant (A) or D3195A mutant (B). Data were fitted to exponential decay processes, and dissociation rate constants were obtained. The gray curve was obtained using the control wt capsids. (C) Ratios between the rate constant obtained for each mutant and the rate constant obtained for the wt control. Values are averages and standard deviations obtained from 2 independent experiments.

capsid pentamers. These residues are located within a surface-exposed region between the 3-fold and 2-fold axes. Removal of the charge of any of those residues (e.g., D3195N; Fig. 1C) by isosteric replacement of the carboxylate by an amide group led to a large stabilization of the virion against thermal dissociation without compromising virus viability. Partial neutralization of the negative charge of those residues by introduction of a positively charged residue nearby (A2065H; Fig. 1C) or charge screening by salt had the same virion-thermostabilizing effect while preserving infectivity (32, 33).
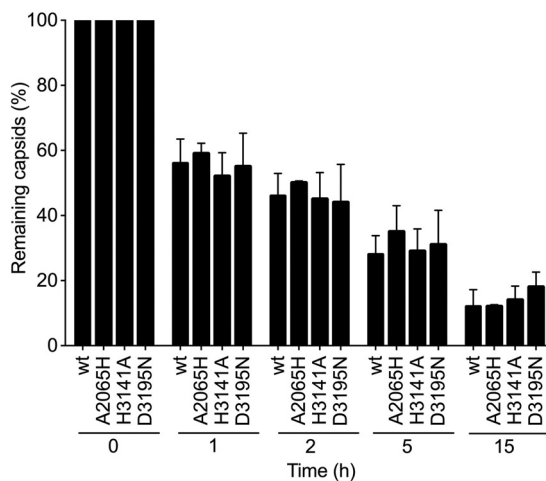

FIG 9 pH sensitivity to dissociation of mutant FMDV empty capsids containing the D3195N, A2065H, or H3141A substitutions relative to that of the wt empty capsid control. The percentages of intact capsids remaining after different incubation times in a representative experiment at pH 5.0 and 25°C are indicated in each case. For each mutant, the average value obtained from 2 independent experiments and the corresponding error bar (standard deviation) are indicated.

As part of the present study, we found that those substitutions (namely, D3195N and A2065H) thermostabilize not only the RNA-filled virion but also the empty capsid. These results showed that the charge-associated thermostabilizing effects of D3195N and A2065H (32, 33) are an intrinsic feature of the FMDV capsid. However, A2065H at least (and probably also D3195N) had a higher thermostabilizing effect on the virion (32, 33) than on the empty capsid under similar conditions (Fig. 7 and 8). This observation suggests that the presence of the charged RNA molecule, in addition to increasing FMDV thermostability, may also modulate the thermostabilizing effect of capsid amino acid substitutions that involve a variation of the electrostatic potential close to the interpentamer interfaces.

Many other amino acid side chains at interpentamer interfaces in the FMDV capsid are charged at neutral pH, but the lethal effect caused by removal of the charged groups prevented an evaluation of their roles on thermostability using virions. In the present study, we analyzed the stability of empty capsids in which several charged groups had been individually removed by substitution to alanine. The results revealed that the determinant role on infectivity of 6 tested residues (all but H3141 and R2018) is not related to any critical role in capsid assembly or thermostability. However, two residues close to each other and to each capsid 2-fold axis, H3141 and R2018, were found to be critical for FMDV infectivity and for limiting capsid thermostability. As indicated in the introduction, both residues may predominantly carry positive charges even at neutral pH and may be involved in repulsive interactions with the positively charged ends of the α-helix dipoles near each capsid 2-fold axis (Fig. 1E).

In summary, two separate regions along the interpentamer interfaces contain charged residues that contribute to keeping the FMDV capsid in a state of remarkably low thermal stability even at neutral pH, most likely through the establishment of electrostatic repulsions involving (i) a cluster of negatively charged residues (D3195 and others) located between the capsid 3-fold and 2-fold axes and (ii) positively charged residues (R2018, H3141) close to each 2-fold axis (Fig. 1).

Is the low intrinsic stability of the FMDV capsid required for preserving virus infectivity? It is generally believed that genome uncoating in FMDV may require disintegration of the virion through dissociation of its capsid into pentameric subunits. Thus, it could be thought that increasing the intrinsic stability of the capsid against full dissociation into pentamers would invariably have a deleterious effect on viral infectivity by impairing the uncoating process. In accord with this view, in this study we identified two amino acid substitutions (R2018A and H3141A) that both stabilize the capsid and are lethal for the virus. However, we also identified other amino acid substitutions (D3195N, A2065H) that equally stabilize the capsid (as well as the virion) but that have no drastic effects on virus infectivity.

The observations made above could be taken as evidence that there may be no relationship between capsid stabilization and impairment of the genome uncoating process required for infection by FMDV. However, it is noteworthy that when the capsid-stabilizing, lethal substitution H3141A was accompanied by the adjacent, charge-restoring N2019H substitution, the latter substitution compensated for the capsid-stabilizing effect of the H3141A substitution and also reversed its lethal effect on the virus. This resulted in a double mutant capsid that was nearly as unstable as the wt capsid and a double mutant virus whose infectivity approached that of the wt virus. This remarkable correlation of effects between capsid thermostability and virus infectivity by compensating mutations strongly argues for a connection between these features.

A hypothesis that is consistent with the ensemble of results obtained here and that is also supported by evidence provided by previous work with different picornaviruses can be proposed. The FMDV genome may exit the virion before the latter is fully disassembled through the transient opening of an energetically weaker region around the 2-fold axis at the center of each interpentamer interface. This local, transient opening could be promoted both by moderate heating *in vitro* or at a constant temperature by acidification in the cell endosomes *in vivo* (by lowering in both cases the free energy barrier

of the opening transition). In turn, this opening transition could be impaired by substitutions (such as H3141A or R2018A) that reduce electrostatic repulsions in this particular region of the interpentamer interface, increasing the free energy barrier of the opening transition and impairing RNA release and virus infectivity.

The evidence for this proposal can be summarized as follows: (i) *in vitro* acidification of equine rhinitis A virus (ERAV), an aphthovirus closely related to FMDV (49, 50), first led to RNA release, leaving an unstable empty capsid that was subsequently disassembled into free pentamers (49). The authors suggested that for ERAV and perhaps also for FMDV, RNA uncoating in the endosomes could proceed by a channel-mediated mechanism, before the capsid is disassembled into pentamers.

(ii) There is strong evidence that the same uncoating mechanism occurs in other picornaviruses, such as human rhinovirus (HRV) and poliovirus (2, 51–54). In these viruses, the viral RNA may leave the capsid through a transient opening located at or close to a capsid 2-fold axis (55, 56).

(iii) When subjected to moderate heating or even during storage at 4°C, FMDV loses infectivity much faster than it is disassembled into pentamers (32). Early studies suggested the presence of an endogenous nuclease inside the FMDV virion that could degrade the RNA on moderate heating (57). However, different amino acid substitutions in the capsid significantly alter the thermal inactivation rate of the virion (32, 58), which indicates that inactivation depends, at least in part, on some intrinsic property of the particle. Exit of the RNA before the capsid is fully dissociated into pentamers is consistent with this observation.

(iv) In this scenario, the differential effects on virus infectivity of different capsid-thermostabilizing substitutions could be consistently explained as follows: stabilizing substitutions R2018A and H3141A (located around each capsid 2-fold axis) could increase the global association energy between pentamers specifically by attenuating local electrostatic repulsions around the genome exit site. In this way a higher temperature would be required *in vitro* or a lower pH would be required *in vivo* to promote the transient opening of a channel at the 2-fold axis, leading to impaired genome uncoating and reduced virus infectivity. In contrast, stabilizing substitutions D3195N and A2065H (located closer to the capsid 3-fold axes) would increase the global association energy between pentamers by attenuating electrostatic repulsions only at regions located far from the genome exit site. In this way, no higher temperature would be required *in vitro* and no lower pH would be required *in vivo* to promote the transient opening through which the RNA is released, preserving normal infectivity.

(v) All four capsid-stabilizing substitutions mentioned above impair the later disassembly of the particle into pentamers, but this effect (though relevant for the development of thermostable vaccines) would be irrelevant for the viral infection process, as the infectivity-determining release of the viral genome would have occurred before the particle is dissociated into pentamers.

This hypothesis predicts that a higher temperature *in vitro* or a higher acidification in the endosomes *in vivo* would be required to release the viral RNA from R2018A and H3141A mutant virions than from the wt and the D3195N and A2065H mutants. In this regard it must be mentioned that no difference in resistance against acid-induced dissociation into pentamers was observed between the H3141A capsid and the wt or the A2065H capsid. However, it is important to remark that the ensemble of ionizable groups that may account for capsid resistance against full pH-induced dissociation into pentamers may include many groups that may not participate in the transient opening of the 2-fold axis regions involved in genome uncoating. Thus, the observed lack of an effect of H3141A on acid-induced capsid dissociation does not mean that this substitution cannot have any effect on genome release before virion disassembly, as predicted by the proposed hypothesis. Unfortunately, the latter prediction cannot be tested because R2018A and H3141A mutant virions cannot be obtained for testing, as these two substitutions are lethal.

The proposed hypothesis, however, also leads to some verifiable predictions. One of these predictions is that substitutions R2018A and H3141A, but not D3195N and

A2065H, should reduce the equilibrium dynamics of the FMDV capsid specifically at the 2-fold axis regions in the interpentamer interfaces.

To sum up, based on the evidence mentioned above, we favor the working hypothesis that genome uncoating in FMDV, as with other picornaviruses, may involve exit of the viral RNA before the capsid fully disassembles into pentamers. Progression of the reaction would eventually lead to complete capsid disassembly, but well after the RNA has been released.

Thermal stabilization of FMDV virions and empty capsids for the development of improved FMD vaccines. A decade ago, we provided the first proof of concept that the FMDV virion can be engineered to become much more stable against heat-induced dissociation, without compromising virus infectivity, genetic stability, sensitivity to chemical inactivation, or antigenic specificity (5, 32, 33). The relevance of these results for improving current, virion-based FMD vaccines has been acknowledged (22). However, other candidate thermostabilizing mutations may compromise virion infectivity and/or genetic stability (32, 33). The results obtained here suggest that the thermostabilization of viruses without losing infectivity (required for vaccine production) may be guided by a better understanding of the effects of mutations on the conformational stabilization of small regions at the interpentamer interfaces that are important during some step of the infectious cycle (e.g., genome uncoating).

The design of stabilizing substitutions for empty capsid-based FMD vaccines is free from constraints related to virus infectivity or genetic stability. In recent years, FMDV empty capsids have been stabilized by introducing either a disulfide bridge (35) or some amino acid substitutions that were predicted to be stabilizing by all-atom molecular dynamics (MD) simulations using a small subset of capsid residues (34, 36). In our case, the predictions of all-atom MD simulations did not generally match the experimentally observed stabilizing effects of the mutations tested here (A. Valbuena and M. G. Mateu, unpublished results). It is important to consider that, in all cases, the free energy difference between the capsid-assembled state and the disassembled state at equilibrium was calculated, whereas dissociation of the FMDV capsid is actually an irreversible process that depends on the activation free energy (i.e., the free energy difference between the assembled state and the transition state of the dissociation reaction) (33). Thus, the effect of amino acid substitutions on capsid stability against irreversible dissociation could be adequately predicted by thermodynamic calculations (such as those undertaken by MD) only when a substitution happens to increase the free energy difference between free and bound pentamers at equilibrium in the same proportion as it increases the activation free energy for irreversible capsid dissociation. Despite the limitations encountered, the ensemble of results obtained holds great promise for the development of thermostabilized vaccines against FMD.

MATERIALS AND METHODS

Plasmids and site-directed mutagenesis. Recombinant empty capsids of FMDV serotype C strain C-S8c1 (wt or mutants) were obtained using plasmids pL1-1 and pSKRH-3C. pL1-1 was derived from pGEM 4Z (Promega) and contains the P1 capsid-coding region of FMDV C-S8c1 plus the first 18 nucleotides of the 2A-coding region under the control of the T7 promoter. pSKRH-3C contains the 3C protease-coding region of FMDV serotype A10 (59). FMDV virions with a C-S8c1 capsid (wt or mutants) were obtained using the infectious plasmid pO1K/C-S8c1 (38, 47). Point mutations were introduced into the FMDV capsid-coding region of plasmid pL1-1 or p3242/C-S8c1 (47) using a QuikChange II XL site-directed mutagenesis kit (Stratagene) following the manufacturer's instructions. The mutagenized segments in p3242/C-S8c1 were subcloned into pO1K/C-S8c1 as previously described (38, 48). The presence of the engineered mutations (and of any other mutation in the capsid-coding region) was determined by automated DNA sequencing.

Recombinant VV. A recombinant vaccinia virus (VV), vTF7-3, that expresses the T7 RNA polymerase (60) was used for the production of FMDV empty capsids as described below. Titration of infectious VV was carried out essentially as previously described (61).

Expression and processing of FMDV capsid proteins and production of empty capsids. BHK-21 cells (in P100 petri dishes at 80% to 90% confluence) were infected with the recombinant VV (61) in Dulbecco's modified Eagle's medium (DMEM) supplemented with nonessential amino acids, antibiotics, and an antifungal and incubated for 1 h at 37°C. For cotransfection of vTF7-3-infected BHK-21 cells with plasmids pL1-1 and pSKRH-3C, a transfection mix was prepared using either mix I or mix

II (the volumes and masses indicated are per P100 dish). Mix I was prepared by diluting 27 μl of the FuGENE 6 reagent (Promega) in DMEM supplemented with nonessential amino acids to a final volume of 600 μl, followed by incubation for 10 min at room temperature (rt); mix II was prepared by diluting 288 μl of cationic liposomes (L-α-phosphatidylethanolamine dioleoyl and dimethyldioctadecyl-ammonium bromide [Sigma], prepared as previously described [61, 62]) in Milli-Q water to a final volume of 600 μl, followed by incubation for 10 min at 4°C. Then, 18 μg of the pL1-1 plasmid and 4.5 μg of the pSKRH-3C plasmid were added to either mix I or mix II, followed by further incubation for 15 min at rt (mix I) or 4°C (mix II).

The infected cells were then washed twice with DMEM (3 ml). Then, DMEM (3 ml) and the transfection mix (600 μl) were added and the cells were incubated for 4 h at 37°C. DMEM (3 ml) supplemented with 10% fetal bovine serum (FBS) was then added, and the cells were incubated for ~16 h at 37°C. The medium was then removed and the cells were washed with phosphate-buffered saline (PBS; 500 μl) and lysed by incubation with ice-cold lysis buffer (500 μl of either 20 mM Tris-HCl, pH 8, 125 mM NaCl, 0.5% NP-40 or 40 mM NaPO$_4$, pH 7.6, 100 mM NaCl, 0.5% NP-40) for 3 min at 4°C.

Capsid protein expression and processing (wt and mutants) were analyzed by SDS-PAGE and Western blotting with a virus protein VP3-specific monoclonal antibody, and the relative amounts of expressed and processed capsid protein were estimated by densitometry. The suspension containing empty capsids was clarified by centrifugation at 14,000 rpm for 10 min at 4°C, and the capsids were purified as described below.

Radiolabeling of FMDV empty capsids. For production of radiolabeled empty capsids, after incubation of the transfected cells for ~16 h the medium was removed, the cells were washed twice with DMEM (5 ml) lacking methionine (Met) and cysteine (Cys), and then DMEM (5 ml) lacking Met and Cys but supplemented with 5% FBS was added. After incubation for 1 h at 37°C, 0.14 mCi of a [^{35}S]Met and Cys amino acid mixture (EasyTag Express 35S protein labeling mix; PerkinElmer) in DMEM lacking Met and Cys (600 μl) was added, and incubation was continued for 2 h at 37°C, before the cells were lysed as described above.

Purification of FMDV empty capsids. Crude cell extracts containing empty capsids were centrifuged through a 20% sucrose cushion (in either TNE buffer [50 mM Tris-HCl, pH 7.5, 5 mM EDTA, 100 mM NaCl] or PN buffer [40 mM sodium phosphate, pH 7.6, 100 mM NaCl) using an SW40 rotor (Beckman Instruments) at 35,000 rpm for 5 h at 4°C. Pellets were resuspended overnight at 4°C in either TNE or PN buffer (400 μl). Preparations of capsids obtained by centrifugation through PN buffer-sucrose cushions were diluted in PN buffer to a final sucrose concentration ranging from 2.2% to 3% sucrose (depending on the experiment), clarified by centrifugation at 14,000 rpm for 30 min at 4°C, and used promptly. If a higher purity was required, partially purified capsids were centrifuged through a 7.5% to 30% sucrose gradient (in TNE buffer) using an SW40 rotor at 37,000 rpm for 3 h at 4°C. The gradients were fractionated into 600-μl aliquots, and fractions containing capsids (sedimentation coefficient, 75S) were pooled, extensively dialyzed against PBS, stored at 4°C, and used promptly.

Electron microscopy. For visualization of empty capsids, samples were deposited on ionized Formvar carbon-coated copper grids (Electron Microscopy Sciences), fixed, washed, and negatively stained, usually with 2% sodium phosphotungstate. The grids were dried and visualized in a JEM-1010 electron microscope (JEOL), and images were recorded using a TemCam F416 camera (TVIPS).

Production of FMDV virions from infectious clones, radiolabeling, purification, titration, and sequencing. FMDV RNA was transcribed from linearized pO1K/C-S8c1 plasmids (wt or mutant) using a Riboprobe in vitro transcription system (Promega) and introduced into BHK-21c2 cells by electroporation essentially as previously described (38, 48). Progeny virions were recovered at different times postelectroporation, generally after a complete cytopathic effect. For comparing infectious virion yields, the same amounts of each mutant RNA and of nonmutated RNA as a control were used in parallel in each experiment. Infectious virus titers were determined in duplicate in standard plaque assays, and the results of 2 or 3 independent experiments were averaged. For metabolic radiolabeling of virions, a [^{35}S]methionine and cysteine amino acid mixture (EasyTag Express ^{35}S protein labeling mix; PerkinElmer) was used essentially as previously described (32).

When needed, virus populations were amplified by up to 3 passages in BHK-21 cell monolayers and titrated again. Virions were purified at 4°C by sedimentation through a sucrose cushion followed by sucrose gradient centrifugation as previously described (32), extensively dialyzed against PBS, and used promptly.

The presence of mutations in progeny virus populations was detected by sequencing of at least the entire capsid coding region. RNA derived from viral populations obtained by electroporation or infection was extracted using the TRIzol reagent LS (Invitrogen) and precipitated with isopropanol. The RNA was reverse transcribed to DNA and amplified by PCR as previously described (38, 48). The DNA products were purified using centrifugal filter units (Amicon Ultra; Millipore) or a Wizard SV gel and PCR clean-up system (Promega) and subjected to automated sequencing.

Analysis of stability of FMDV empty capsids and virions against thermally induced dissociation at neutral pH. The stability of empty capsids and virions against thermal dissociation into pentamers was determined essentially as previously described (32). Briefly, partially or highly purified, radiolabeled empty capsids or virions in either PBS (pH 7.5) (for purified viral particles) or PN buffer with 2.2% to 3% sucrose (for partially purified capsids) were incubated at 42°C for different amounts of time. Every experiment included wt virions or empty capsids as an internal control. To stop the disassembly reaction, samples were transferred to ice at selected time points. The amount of remaining capsids or virions at each incubation time point was estimated by centrifugation in sucrose gradients and determination of the radioactivity present in each fraction. For virion samples we used 7.5% to 45% sucrose gradients in

TNE buffer at 18,000 rpm for 18 h at 4°C. For capsid samples, we used either 7.5% to 45% sucrose gradients in TNE buffer at 18,000 rpm for 18 h at 4°C or 7.5% to 30% sucrose gradients in PN buffer at 35,000 rpm for 3.5 h at 4°C. In each experiment with either mutant capsids or virions, the wt capsids or virions, as appropriate, were included as an internal control to compare thermal stability, in parallel, under exactly the same conditions. The results obtained for the mutant virus particles were normalized with respect to those obtained for the wt virus particles in the same experiment. For kinetic analysis, the fraction of intact capsids or virions remaining was plotted against the incubation time and fitted to an exponential decay to estimate the dissociation rate constant.

Analysis of stability of FMDV empty capsids against acid-induced dissociation. The stability of empty capsids against acid-induced dissociation was determined essentially as previously described (21, 58). Briefly, suspensions of partially purified radiolabeled empty capsids in PBS (pH 7.5; 150 μl) were acidified to pH 5.0 by addition of citrate buffer (50 mM citrate at pH 5.0, 140 mM NaCl; 50 μl) and incubated for different amounts of time at 25°C. After incubation, the pH was raised to 7.5 by addition of 30 μl of 1 M Tris-HCl, pH 8.5. The pHs were verified by direct measurement with a microelectrode. Then, the amount of capsids at each time point was estimated by centrifugation in sucrose gradients (7.5% to 30% sucrose in PN buffer) at 35,000 rpm for 3.5 h at 4°C and determination of the radioactivity present in each fraction. In each experiment, the wt capsid was included as an internal control to compare stability in parallel under exactly the same conditions. The results obtained for each mutant capsid were normalized with respect to those for the wt capsid in the same experiment.

Computational structural analyses. The Protein Data Bank (PDB) atomic coordinates for the crystal structure of FMDV C-S8c1 (PDB accession number 1FMD) (37) were inspected graphically using VMD software (63). Contact and solvent accessibility analyses were performed using WHAT IF software (64).

REFERENCES

1. Johnson JE. 2003. Virus particle dynamics. Adv Protein Chem 64:197–218. https://doi.org/10.1016/S0065-3233(03)01005-2.
2. Bothner B, Hilmer JK. 2011. Probing viral capsids in solution, p 41–61. In Agbandje-McKenna M, McKenna R(ed), Structural virology. RSC Publishing, Cambridge, United Kingdom.
3. Veesler D, Johnson JE. 2012. Virus maturation. Annu Rev Biophys 41:473–496. https://doi.org/10.1146/annurev-biophys-042910-155407.
4. Mateu MG. 2013. Assembly, stability and dynamics of virus capsids. Arch Biochem Biophys 532:65–79. https://doi.org/10.1016/j.abb.2012.10.015.
5. Mateu MG. 2017. The foot-and-mouth disease virion: structure and function, p 61–105. In Sobrino F, Domingo E(ed), Foot-and-mouth disease virus. Caister Academic Press, Norfolk, United Kingdom.
6. Yuan H, Li P, Ma X, Lu Z, Sun P, Bai X, Zhang J, Bao H, Cao Y, Li D, Fu Y, Chen Y, Bai Q, Zhang J, Liu Z. 2017. The pH stability of foot-and-mouth disease virus. Virol J 14:233. https://doi.org/10.1186/s12985-017-0897-z.
7. Zlotnick A, Fane BA. 2011. Mechanisms of icosahedral virus assembly, p 180–202. In Agbandje-McKenna M, McKenna R(ed), Structural virology. RSC Publishing, Cambridge, United Kingdom.
8. Valbuena A, Rodriguez-Huete A, Mateu MG. 2018. Mechanical stiffening of human rhinovirus by cavity-filling antiviral drugs. Nanoscale 10:1440–1452. https://doi.org/10.1039/C7NR08704G.
9. Suomalainen M, Greber UF. 2013. Uncoating of non-enveloped viruses. Curr Opin Virol 3:27–33. https://doi.org/10.1016/j.coviro.2012.12.004.
10. Perlmutter JD, Hagan MF. 2015. Mechanisms of virus assembly. Annu Rev Phys Chem 66:217–239. https://doi.org/10.1146/annurev-physchem-040214-121637.
11. Douglas TA, Young M. 2006. Viruses: making friends with old foes. Science 312:873–875. https://doi.org/10.1126/science.1123223.
12. Wen AM, Rambhia PH, French RH, Steinmetz NF. 2013. Design rules for nanomedical engineering: from physical virology to the applications of virus-based materials in medicine. J Biol Phys 39:301–325. https://doi.org/10.1007/s10867-013-9314-z.
13. Mateu MG. 2016. Assembly, engineering and application of virus-based protein nanoparticles, p 83–120. In Cortajarena AL, Grove TZ(ed), Protein-based engineered nanostructures. Springer, Basel, Switzerland.
14. Hill BD, Zak A, Khera E, Wen F. 2018. Engineering virus-like particles for antigen and drug delivery. Curr Protein Pept Sci 19:112–127. https://doi.org/10.2174/1389203718666161122113041.
15. Jamal SM, Belsham GJ. 2013. Foot-and-mouth disease: past, present and future. Vet Res 44:116. https://doi.org/10.1186/1297-9716-44-116.
16. Sobrino F, Domingo E (ed). 2017. Foot-and-mouth disease virus. Caister Academic Press, Norfolk, United Kingdom.
17. Acharya R, Fry E, Stuart D, Fox G, Rowlands D, Brown F. 1989. The three-dimensional structure of foot-and-mouth disease virus at 2.9 Å resolution. Nature 337:709–716. https://doi.org/10.1038/337709a0.
18. Fry EE, Stuart Dl. 2010. Virion structure, p 59–72. In Ehrenfeld E, Domingo E, Roos RP(ed), The picornaviruses. ASM Press, Washington, DC.
19. Carrillo EC, Giachetti C, Campos RH. 1985. Early steps in FMDV replication: further analysis on the effects of chloroquine. Virology 147:118–125. https://doi.org/10.1016/0042-6822(85)90232-6.
20. Baxt B. 1987. Effect of lysosomotropic compounds on early events in foot-and-mouth disease virus replication. Virus Res 7:257–271. https://doi.org/10.1016/0168-1702(87)90032-3.
21. Martín-Acebes MA, Rincón V, Armas-Portela R, Mateu MG, Sobrino F. 2010. A single amino acid substitution in the capsid of foot-and-mouth disease virus can increase acid lability and confer resistance to acid-dependent uncoating inhibition. J Virol 84:2902–2912. https://doi.org/10.1128/JVI.02311-09.

22. Hegde NR, Maddur MS, Rao PP, Kaveri SV, Bayry J. 2009. Thermostable foot-and-mouth disease virus as a vaccine candidate for endemic countries: a perspective. Vaccine 27:2199–2201. https://doi.org/10.1016/j.vaccine.2009.01.032.

23. Rowlands DJ. 2017. Introduction: foot-and-mouth disease-much progress but still a lot to learn, p 1–12. In Sobrino F, Domingo E(ed), Foot-and-mouth disease virus. Caister Academic Press, Norfolk, United Kingdom.

24. Vallat B, Domenech J, Schudel AA. 2017. The role of international organizations in the control of foot-and-mouth disease, p 409–416. In Sobrino F, Domingo E(ed), Foot-and-mouth disease virus. Caister Academic Press, Norfolk, United Kingdom.

25. Smitsaart EN, Bergmann I. 2017. Quality attributes of current inactivated foot-and-mouth disease vaccines and their effects on the success of vaccination programmes, p 287–316. In Sobrino F, Domingo E(ed), Foot-and-mouth disease virus. Caister Academic Press, Norfolk, United Kingdom.

26. Doel TR, Baccarini PJ. 1981. Thermal stability of foot-and-mouth disease virus. Arch Virol 70:21–32. https://doi.org/10.1007/BF01320790.

27. Doel TR, Chong WK. 1982. Comparative immunogenicity of 146S, 75S and 12S particles of foot-and-mouth disease virus. Arch Virol 73:185–191. https://doi.org/10.1007/BF01314726.

28. Roosien J, Belsham GJ, Ryan MD, King AM, Vlak JM. 1990. Synthesis of foot-and-mouth disease virus capsid proteins in insect cells using baculovirus expression vectors. J Gen Virol 71:1703–1711. https://doi.org/10.1099/0022-1317-71-8-1703.

29. Lewis SA, Morgan DO, Grubman M. 1991. Expression, processing and assembly of foot-and-mouth disease virus capsid structures in heterologous systems: induction of a neutralizing antibody response in guinea pigs. J Virol 65:6572–6580.

30. Abrams CC, King AM, Belsham GJ. 1995. Assembly of foot-and-mouth disease virus empty capsids synthesized by a vaccinia virus expression system. J Gen Virol 76:3089–3098. https://doi.org/10.1099/0022-1317-76-12-3089.

31. Dong H, Guo HC, Sun SQ. 2014. Virus-like particles in picornavirus vaccine development. Appl Microbiol Biotechnol 98:4321–4329. https://doi.org/10.1007/s00253-014-5639-1.

32. Mateo R, Luna E, Rincón V, Mateu MG. 2008. Engineering viable foot-and-mouth disease viruses with increased thermostability as a step in the development of improved vaccines. J Virol 82:12232–12240. https://doi.org/10.1128/JVI.01553-08.

33. Rincón V, Rodríguez-Huete A, López-Argüello S, Ibarra-Molero B, Sanchez-Ruiz JM, Harmsen MM, Mateu MG. 2014. Identification of the structural basis of thermal lability of a virus provides a rationale for improved vaccines. Structure 22:1560–1570. https://doi.org/10.1016/j.str.2014.08.019.

34. Scott KA, Kotecha A, Seago J, Ren J, Fry EE, Stuart DI, Charleston B, Maree FF. 2017. SAT2 foot-and-mouth disease virus structurally modified for increased thermostability. J Virol 91:e02312-16. https://doi.org/10.1128/JVI.02312-16.

35. Porta C, Kotecha A, Burman A, Jackson T, Ren J, Loureiro S, Jones IM, Fry EE, Stuart DI, Charleston B. 2013. Rational engineering of recombinant picornavirus capsids to produce safe, protective vaccine antigen. PLoS Pathog 9:e1003255. https://doi.org/10.1371/journal.ppat.1003255.

36. Kotecha A, Seago J, Scott K, Burman A, Loureiro S, Ren J, Porta C, Ginn HM, Jackson T, Perez-Martin E, Siebert CA, Paul G, Huiskonen JT, Jones IM, Esnouf RM, Fry EE, Maree FF, Charleston B, Stuart DI. 2015. Structure-based energetics of protein interfaces guides foot-and-mouth disease virus vaccine. Nat Struct Mol Biol 22:788–794. https://doi.org/10.1038/nsmb.3096.

37. Lea S, Hernández J, Blakemore W, Brocchi E, Curry S, Domingo E, Fry E, Abu-Ghazaleh R, King AMQ, Newman J, Stuart D, Mateu MG. 1994. The structure and antigenicity of a serotype C foot-and-mouth disease virus. Structure 2:123–139. https://doi.org/10.1016/S0969-2126(00)00014-9.

38. Mateo R, Diaz A, Baranowski E, Mateu MG. 2003. Complete alanine scanning of intersubunit interfaces in a foot-and-mouth disease virus capsid reveals critical contributions of many side chains to particle stability and viral function. J Biol Chem 278:41019–41027. https://doi.org/10.1074/jbc.M304990200.

39. Inagaki F, Kawano Y, Shimada I, Takahashi K, Miyazawa T. 1981. Nuclear magnetic resonance study of the microenvironments of histidine residues of ribonuclease T1 and carboxymethylated ribonuclease T1. J Biochem 89:1185–1195.

40. Anderson DE, Becktel WJ, Dahlquist FW. 1990. pH-induced denaturation

41. of proteins: a single salt bridge contributes 3-5 kcal/mol to the free energy of folding of T4 lysozyme. Biochemistry 29:2403–2408. https://doi.org/10.1021/bi00461a025.

41. Curry S, Abrams CC, Fry E, Crowther JC, Belsham GJ, Stuart DI, King AM. 1995. Viral RNA modulates the acid sensitivity of foot-and-mouth disease virus capsids. J Virol 69:430–438.

42. Twomey T, France LL, Hassard S, Burrage TG, Newman JF, Brown F. 1995. Characterization of acid-resistant mutant of foot-and-mouth disease virus. Virology 206:69–75. https://doi.org/10.1016/S0042-6822(95)80020-4.

43. Curry S, Fry E, Blakemore W, Abu-Ghazaleh R, Jackson T, King A, Lea S, Newman J, Stuart D. 1997. Dissecting the roles of VP0 cleavage and RNA packaging in picornavirus capsid stabilization: the structure of empty capsids of foot-and-mouth disease virus. J Virol 71:9743–9752.

44. van Vlijmen HWT, Curry S, Schaefer M, Karplus M. 1998. Titration calculations of foot-and-mouth disease virus capsids and their stabilities as a function of pH. J Mol Biol 275:295–308. https://doi.org/10.1006/jmbi.1997.1418.

45. Ellard FM, Drew J, Blakemore WE, Stuart DI, King A. 1999. Evidence for the role of His-142 of protein 1C in the acid-induced disassembly of foot-and-mouth disease virus capsids. J Gen Virol 80:1911–1918. https://doi.org/10.1099/0022-1317-80-8-1911.

46. Luna E, Rodríguez-Huete A, Rincón V, Mateo R, Mateu MG. 2009. Systematic study of the genetic response of a variable virus to the introduction of deleterious mutations in a functional capsid region. J Virol 83:10140–10151. https://doi.org/10.1128/JVI.00903-09.

47. Baranowski E, Sevilla N, Verdaguer N, Ruiz-Jarabo CM, Beck E, Domingo E. 1998. Multiple virulence determinants of foot-and-mouth disease virus in cell culture. J Virol 72:6362–6372.

48. Mateo R, Mateu MG. 2007. Deterministic, compensatory mutational events in the capsid of foot-and-mouth disease virus in response to the introduction of mutations found in viruses from persistent infections. J Virol 81:1879–1887. https://doi.org/10.1128/JVI.01899-06.

49. Tuthill TJ, Harlos K, Walter TS, Knowles NJ, Groppelli E, Rowlands DJ, Stuart DI, Fry EE. 2009. Equine rhinitis A virus and its low pH empty particle: clues towards an aphthovirus entry mechanism? PLoS Pathog 5:e1000620. https://doi.org/10.1371/journal.ppat.1000620.

50. Groppelli E, Tuthill TJ, Rowlands DJ. 2010. Cell entry of the aphthovirus equine rhinitis A virus is dependent on endosome acidification. J Virol 84:6235–6240. https://doi.org/10.1128/JVI.02375-09.

51. Lewis JK, Bothner B, Smith TJ, Siuzdak G. 1998. Antiviral agent blocks breathing of the common cold virus. Proc Natl Acad Sci U S A 95:6774–6778. https://doi.org/10.1073/pnas.95.12.6774.

52. Kolatkar PR, Bella J, Olson NH, Bator CM, Baker TS, Rossmann MG. 1999. Structural studies of two rhinovirus serotypes complexed with fragments of their cellular receptor. EMBO J 18:6249–6259. https://doi.org/10.1093/emboj/18.22.6249.

53. Hogle JM. 2002. Poliovirus cell entry: common structural themes in viral cell entry pathways. Annu Rev Microbiol 56:677–702. https://doi.org/10.1146/annurev.micro.56.012302.160757.

54. Ehrenfeld E, Domingo E, Roos RP (ed). 2010. The picornaviruses. ASM Press, Washington, DC.

55. Bostina M, Levy D, Filman J, Hogle J. 2011. Poliovirus RNA is released from the capsid near a twofold symmetry axis. J Virol 85:776–783. https://doi.org/10.1128/JVI.00531-10.

56. Garriga D, Pickl-Herk A, Luque D, Wruss J, Castón JR, Blaas D, Verdaguer N. 2012. Insights into minor group rhinovirus uncoating: the X-ray structure of the HRV2 empty capsid. PLoS Pathog 8:e1002473. https://doi.org/10.1371/journal.ppat.1002473.

57. Brown F, Wild TF. 1966. The effect of heat on the structure of foot-and-mouth disease virus and the viral ribonucleic acid. Biochim Biophys Acta 119:301–308. https://doi.org/10.1016/0005-2787(66)90188-2.

58. Martín-Acebes MA, Vázquez-Calvo A, Rincón V, Mateu MG, Sobrino F. 2011. A single amino acid substitution in the capsid of foot-and-mouth disease virus can increase acid resistance. J Virol 85:2733–2740. https://doi.org/10.1128/JVI.02245-10.

59. Belsham GJ, McInerney GM, Ross-Smith N. 2000. Foot-and-mouth disease virus 3C protease induces cleavage of translation initiation factors eIF4A and eIF4G within infected cells. J Virol 74:272–280. https://doi.org/10.1128/JVI.74.1.272-280.2000.

60. Fuerst TR, Niles EG, Studier FW, Moss B. 1986. Eukaryotic transient-expression system based on recombinant vaccinia virus that synthesizes bacteriophage T7 RNA polymerase. Proc Natl Acad Sci U S A 83:8122–8126. https://doi.org/10.1073/pnas.83.21.8122.

61. Martínez-Salas E, Saiz JC, Dávila M, Belsham GJ, Domingo E. 1993. A

single nucleotide substitution in the internal ribosome entry site of foot-and-mouth disease virus leads to enhanced cap-independent translation in vivo. J Virol 67:3748–3755.

62. Rose JK, Buonocore L, Whitt MA. 1991. A new cationic liposome reagent mediating nearly quantitative transfection of animal cells. Biotechniques 10:520–525.

63. Humphrey W, Dalke A, Schulten K. 1996. VMD: visual molecular dynamics. J Mol Graph 14:33–38. https://doi.org/10.1016/0263-7855(96)00018-5.

64. Vriend G. 1990. WHAT IF: a molecular modeling and drug design program. J Mol Graph 8:52–56. https://doi.org/10.1016/0263-7855(90)80070-V.